Strahlenther Onkol (2018) 194:929–943
https://doi.org/10.1007/s00066-018-1349-4

ORIGINAL ARTICLE

Stereotactic radiotherapy for choroidal melanomas by means of HybridArc™

Physics and technique of linac-based photon beam therapy

Markus Wösle[1] · Lothar Krause[2] · Shanthala Sreenivasa[1,3] · Dirk Vordermark[4] · Ilja F. Ciernik[1]

Received: 28 January 2018 / Accepted: 2 August 2018 / Published online: 16 August 2018

Abstract

Purpose Stereotactic radiotherapy (SRT) is suitable to treat ocular tumours. The optimal beam geometry for SRT, however, has not been defined. Here we evaluate a combination technique with dynamic conformal arcs (DCAs) and intensity-modulated static fields (IMRT), known as HybridArc™ (HA).

Methods For the first consecutive 25 cases with choroidal melanomas with volumes of 0.02 to 1.18 cm^3 treated with 50 Gy in five fractions, the results with respect to dose conformity, homogeneity, and dose distributions were summarised. To describe the dose distribution at the planning target volume (PTV) boundary, we defined a spatially averaged dose gradient (SADG) and compared it with Paddick's gradient index (GI). We made dosimetric comparisons between HA and other irradiation techniques.

Results The PTVs ranged from 0.42 to 3.37 cm^3. The conformity index (CI) was 1.25 ± 0.15, and the homogeneity index (HI) 0.08 ± 0.02. The SADG was (–3.5 ± 0.5) Gy/mm or (–7.0 ± 1.0) %/mm between the isodose levels 95 and 20%; local minima reached –11.5 Gy/mm or –22.9%/mm. The coefficient of determination for a nonlinear regression of GI on SADG was 0.072. After a median follow-up time of 19.6 months, local tumour control was 100% without any case of post-therapeutic enucleation. Two patients (8%) developed liver metastases.

Conclusion SRT of ocular tumours by HA is highly appropriate, and HA is superior to intensity-modulated arc therapy (IMAT) concerning dose reduction in organs at risk (OARs). The novel gradient measure SADG is more informative than Paddick's GI.

Keywords Ocular tumour · Eye-preserving therapy · Hybrid irradiation technique · Spatially averaged dose gradient · Ophthalmological marker

✉ Dr.-Ing. Markus Wösle, M. Sc.
markus.woesle@klinikum-dessau.de

[1] Klinik für Strahlentherapie und Radioonkologie, Städtisches Klinikum Dessau, Auenweg 38, 06847 Dessau-Roßlau, Germany

[2] Klinik für Augenheilkunde und Zentrum für Refraktive Chirurgie, Städtisches Klinikum Dessau, Auenweg 38, 06847 Dessau-Roßlau, Germany

[3] Medizinische Fakultät, Martin-Luther-Universität Halle-Wittenberg, Magdeburger Straße 8, 06108 Halle (Saale), Germany

[4] Universitätsklinik und Poliklinik für Strahlentherapie, Universitätsklinikum Halle (Saale), Ernst-Grube-Straße 40, 06120 Halle (Saale), Germany

Stereotaktische Radiotherapie von Aderhautmelanomen mittels HybridArc™

Physik und Technik der linearbeschleunigerbasierten Photonentherapie

Zusammenfassung

Zielsetzung Die stereotaktische Radiotherapie (SRT) ist zur Behandlung von Augentumoren geeignet. Jedoch ist bis jetzt noch keine Definition der optimalen Bestrahlungsgeometrie zur SRT erfolgt. Wir bewerten hier eine kombinierte Bestrahlungstechnik, bestehend aus dynamischen konformalen Rotationsfeldern (DCAs) und intensitätsmodulierten statischen Feldern (IMRT), die als HybridArc™ (HA) bekannt ist.

Methoden Für die ersten 25 aufeinanderfolgenden Fälle mit Aderhautmelanomen in einem Volumenbereich von 0,02 bis 1,18 cm^3, die mit 50 Gy in fünf Fraktionen bestrahlt wurden, wurden die Ergebnisse bezüglich Dosiskonformität, Dosishomogenität und Dosisverteilungen zusammengefasst. Zur Beschreibung der Dosisverteilung am Zielvolumenrand wurde ein räumlich gemittelter Dosisgradient (SADG) definiert und mit dem Gradientenindex (GI) nach Paddick verglichen. Wir stellten dosimetrische Vergleiche zwischen HA und anderen Bestrahlungstechniken an.

Ergebnisse Die Planungszielvolumina (PTVs) lagen im Größenbereich von 0,42 bis 3,37 cm^3. Für den Konformitätsindex (CI) und den Homogenitätsindex (HI) waren die Werte 1,25 ± 0,15 bzw. 0,08 ± 0,02. Der SADG betrug –3,5 ± 0,5 Gy/mm bzw. –7,0 ± 1,0 %/mm zwischen den Isodosenniveaus 95 und 20 %; lokale Minima erreichten –11,5 Gy/mm bzw. –22,9 %/mm. Der Determinationskoeffizient einer nichtlinearen Regression von GI über SADG war 0,072. Nach einem medianen Nachbeobachtungszeitraum von 19,6 Monaten lag die lokale Tumorkontrollrate bei 100 %, ohne einen einzigen Fall einer posttherapeutischen Enukleation. Zwei Patienten (8 %) entwickelten Lebermetastasen.

Schlussfolgerung Die SRT von Augentumoren mittels HA ist äußerst gut geeignet. HA ist der intensitätsmodulierten Rotationstherapie (IMAT) bezüglich der Dosiseinsparung in Risikoorganen (OARs) überlegen. Das neu eingeführte Gradientenmaß SADG besitzt gegenüber dem GI nach Paddick mehr Informationsgehalt.

Schlüsselwörter Augentumor · Augenerhaltende Therapie · Hybride Bestrahlungstechnik · Räumlich gemittelter Dosisgradient · Ophthalmologischer Marker

Introduction

Primary ocular tumours are rare diseases with a reported incidence rate with age standardisation of $1.42 \cdot 10^{-5}$ in Germany in 2014 [1]. Current therapies include enucleation, and organ-preserving therapies now are used for the vast majority of patients, such as brachytherapy [2–4], proton beam therapy (PBT; [5]), the Leksell Gamma Knife® (Elekta Instrument AB, Stockholm, Sweden; [6]), linac-based stereotactic radiotherapy (SRT; [7]) or robotic stereotactic radiosurgery (SRS) by CyberKnife® (Accuracy, Sunnyvale, CA, USA; [8]). In combination with surgical therapies, such as transscleral exoresection, transretinal endoresection and transpupillary thermotherapy, radiation therapy generally ascertains high rates of local tumour control and eye preservation [9]. Jang et al. recently reported that radiotherapy alone may provide a survival advantage over surgical resection alone [10].

Eye tumours are generally small, subjected to movements and located close to several radiation-sensitive organs. Radiation-induced side effects are dry eye syndrome, keratitis, cataract, optic neuropathy, glaucoma, retinopathy and retinal detachment. Therefore, highly conformal dose distributions with steep dose gradients are mandatory. The effectiveness and safety of PBT sets the gold standard for curative radiotherapy of ocular tumours [11]. However, the choice of treatment modality should be considered carefully, as in some situations, alternative irradiation techniques might be preferred to PBT [12].

Thus, since the clinical introduction of stereotactic photon beam therapy and SRS, external photon beams have been successfully used, pioneered by the Medical University of Vienna. 212 patients with choroidal melanomas from 1997 to 2007, not suitable for brachytherapy, were treated by means of SRT with 6 MV photons of a linear accelerator, and 50, 60 or 70 Gy were delivered with five fractions within one week. The local tumour control was 92.6% after 10 years. 32 patients (15.1%) developed metastatic disease, and 22 (10.4%) of these patients died during the follow-up period [7].

Alternative external photon beam techniques have been reported for the Gamma Knife® [6] and the CyberKnife® [13, 14]. The use of the Gamma Knife® with single-fraction marginal dose values between 40 and 80 Gy (median 50 Gy) resulted in an increased risk of retinopathy when treating large tumour volumes [15]. In 2016, a series of 217 patients with medium and large uveal melanomas treated by means of a CyberKnife® were published [8]. 3.3% of the treated tumours were small (size classification T1 or T2), 66.9% of medium (T2 or T3), and 29.8% of large size (T3 or T4). Single-fraction frameless radiosurgery using image guidance was used with a dose in the range of 18 to 22 Gy. The

local control rates at 3 and 5 years were 87.4 and 70.8%, respectively; the corresponding values of the eye-preserving rate were 86.7 and 73.0%, respectively.

In the present article, we examined how to maximise dose conformity and optimise dose to organs at risk (OARs) for ocular tumours by using dynamic conformal arcs (DCAs) complemented with additional intensity-modulated static fields (IMRT). We present the performance of this combination technique, known as HybridArc™ (HA; [16]), with respect to the creation of highly conformal dose distributions and steep dose gradients at the tumour's boundary, as well as good dose homogeneity in the target volume with a low output dose. 25 cases with choroidal melanomas, treated with 50 Gy in five fractions, were included in our study. The minimal safety margins for image-guided radiotherapy (IGRT) with four implanted ophthalmological markers, closed eyes, frameless radiosurgery system, and six-dimensional (six-D) positioning corrections were determined. Dose conformity and dose homogeneity for the target volume, as well as dose distributions in the tumour and OARs were analysed. To describe the dose drop-off at the target volume boundary towards normal tissue, we defined and brought into use a spatially averaged dose gradient (SADG) and compared it with the gradient index (GI) of Paddick et al. [17]. Once again, we assessed the dose distributions of all cases related to SADG. Moreover, we described the dose delivery by a stereotactic linear accelerator and the appertaining quality assurance procedures. The results of treatment planning and clinical outcome were compared with previously published data.

Materials and methods

From all treated patients with choroidal tumours since 2014, we evaluated a cohort of the first 25 cases with malignant choroidal melanomas with a planning target volume (PTV) not exceeding the half volume of the eye and treated with 50 Gy delivered in five fractions within one week. For the purpose of target localisation and IGRT, implanted ophthalmological markers were used. The gross tumour volumes (GTVs) were (0.56 ± 0.40) cm^3 (range of 0.02 to 1.18 cm^3); here and in the following, a quantity is characterised by two pairs of values: mean value plus/minus standard deviation and range in brackets. The age in this group was 30 to 91 years (median 69 years) at the date of first diagnosis.

Patients and tumours

Table 1 contains the patients' characteristics. The percentage distribution of tumour size classifications showed 24% T1a, 12% T2a, 40% T3(a or b) and 24% T4(a or b). The classification of lymph node involvement was N0 and of distant metastatic spread M0 for all patients. The octants of

Table 1 Patients' characteristics: age, tumour classification, tumour location and tumour size of 25 patients with choroidal melanomas, irradiated in the years 2015 and 2016

Patient no.	Age[a] [years]	AJCC[b] classification	COMS[c] classification	Eye	Octant[d]	Papilla infiltration[e]	a_P [mm]	a_M [mm]	a_{LG} [mm]	b_{max} [mm]	t [mm]	GTV [cm^3]
1	79	T3a N0 M0	Medium	Right	VIII	No	2.8	5.0	13.2	15.9	7.9	0.53
2	42	T4a N0 M0	Large	Left	VII, VIII	No	3.7	2.9	6.2	18.4	6.0	0.56
3	84	T1a N0 M0	Medium	Left	III, VII	Yes	0.0	2.9	11.7	7.9	3.5	0.07
4	62	T1a N0 M0	Medium	Left	VIII	No	1.2	1.6	8.5	7.7	4.0	0.10
5	86	T4a N0 M0	Large	Left	IV, VIII	Yes	0.0	1.2	4.0	18.4	6.6	0.90
6	68	T3a N0 M0	Medium	Left	III, VII	Yes	0.0	0.9	13.8	13.6	6.3	0.42
7	60	T4a N0 M0	Large	Left	IV	Yes	0.0	0.0	2.0	19.6	6.8	1.05
8	79	T3b N0 M0	Large	Left	V, VI	No	11.2	10.9	7.0	16.2	10.2	1.10
9	76	T3a N0 M0	Large	Right	VIII	No	1.7	4.3	20.4	16.4	10.1	0.83
10	75	T4a N0 M0	Large	Right	VII, VIII	No	1.3	0.9	2.4	18.8	8.2	1.15
11	78	T2a N0 M0	Medium	Left	III, VII	No	1.3	4.3	16	9.3	5.5	0.20

Table 1 (Continued)

Patient no.	Age[a] [years]	AJCC[b] classification	COMS[c] classification	Eye	Octant[d]	Papilla infiltration[e]	a_P [mm]	a_M [mm]	a_{LG} [mm]	b_{max} [mm]	t [mm]	GTV [cm^3]
12	52	T2a N0 M0	Medium	Left	IV	Yes	0.0	0.0	5.1	10.9	3.4	0.20
13	30	T3a N0 M0	Large	Right	VII, VIII	Yes	0.0	0.7	5.0	11.4	9.2	0.49
14	58	T2a N0 M0	Medium	Right	VII	No	1.7	3.1	1.0	12.2	3.9	0.18
15	70	T3b N0 M0	Medium	Right	VI, VII	No	2.4	2.5	4.4	15.6	9.3	0.87
16	55	T1a N0 M0	Medium	Right	IV	No	2.1	7.0	16.1	8.8	4.6	0.12
17	59	T1a N0 M0	Medium	Left	IV, VIII	Yes	0.0	1.2	3.9	11.7	2.8	0.18
18	77	T3a N0 M0	Medium	Left	III, IV, VIII	Yes	0.0	0.8	5.9	15.2	3.1	0.21
19	75	T1a N0 M0	Medium	Left	VII, VIII	Yes	0.0	0.9	9.9	7.6	3.8	0.11
20	72	T1a N0 M0	Small	Left	VII, VIII	No	1.1	1.4	11.4	7.3	1.3	0.02
21	91	T3a N0 M0	Medium	Left	VII	Yes	0.0	1.0	10.1	15.0	7.5	0.53
22	41	T3b N0 M0	Medium	Left	VI, VII	No	1.7	4.8	17.6	16.0	9.6	0.84
23	61	T4b N0 M0	Large	Left	VI, VII, VIII	Yes	0.0	6.0	10.8	19.5	11.1	1.01
24	46	T3a N0 M0	Large	Right	II, III	No	1.4	2.1	0.0	18.0	10.1	1.08
25	69	T4a N0 M0	Large	Left	III, VII	Yes	0.0	0.9	11.7	18.6	10.3	1.18
Mean value							1.5	2.7	8.7	14	6.6	0.56
Standard deviation							2.2	2.6	5.5	4.2	2.9	0.40

a_P minimal distance between tumour and ipsilateral papilla; a_M minimal distance between tumour and ipsilateral macula lutea; a_{LG} minimal distance between tumour and ipsilateral lacrimal gland; b_{max} maximal basal diameter of the tumour; *t* tumour's thickness; *GTV* gross tumour volume

[a]Patient's age at the date of primary diagnosis

[b]TNM staging system for melanomas of the eye by the American Joint Committee on Cancer (AJCC)

[c]Size classification scheme for choroidal melanomas according to the Collaborative Ocular Melanoma Study Group (COMS)

[d]The octants of the eyeball are numbered according to Fig. 1

[e]Ophthalmologist's diagnosis

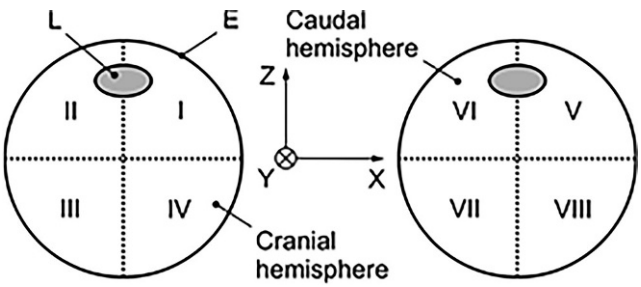

Fig. 1 Schematic segmentation of the eyeball in eight octants: I–IV in the cranial and V–VIII in the caudal hemisphere. *E* equator line; *L* cross-section of the lens in the eye's equatorial plane; *X, Y, Z* system of coordinates represents the anatomical orientations right-to-left, inferior-to-superior and posterior-to-anterior, respectively

tumour location in Table 1 are illustrated in Fig. 1. According to the size classification scheme of the Collaborative Ocular Melanoma Study Group (COMS), 4% small, 56% medium and 40% large tumours were included in our cohort [18]. The first data row of Table 2 shows that tiny and large tumours with a median PTV size of 1.84 cm^3 are included in our study. The average volume of an adult's eye is 7.24 cm^3. 48% of all tumours infiltrated the optic disc area.

Treatment planning

The standard imaging modalities for tumour segmentation and treatment planning are fundus photography, sonography, native computer tomography, as well as T1-weighted

Table 2 Treatment planning parameters of 25 planning target volumes (PTVs)

Property/criterion	Minimum	Maximum	Mean value	Standard deviation
V_{PTV} [cm^3]	0.42	3.37	1.83	0.98
$V_{90\%}$ [%]	96.7	100.0	99.5	0.8
$V_{95\%}$ [%]	93.9	100.0	97.8	1.8
D_{min} [%]	71.3	96.1	86.0	7.7
$D_{98\%}$ [%]	89.3	97.7	94.3	2.3
D_{mean} [%]	99.2	100.1	99.7	0.3
$D_{50\%}$ [%]	100.0	101.0	100.5	0.2
$D_{2\%}$ [%]	101.4	103.1	102.2	0.4
D_{max} [%]	101.7	105.1	103.2	0.9
$CI_{95\%}$ [1]	1.07	1.66	1.25	0.15
HI [1]	0.04	0.13	0.08	0.02
IC [1]	0.06	0.47	0.21	0.12
$SADG\|_{10\,Gy}^{47.5\,Gy}$ [Gy/mm]	–4.6	–2.6	–3.5	0.5
$SADG\|_{43\,\%}^{86\,\%}$ [%/mm]	–17.3	–9.0	–11.9	2.1
GI [1]	2.4	3.8	2.9	0.3
$(D_{out}/D_{nom})_{DCA}$ [MU/cGy]	1.26	1.69	1.45	1.10
$(D_{out}/D_{nom})_{IMRT}$ [MU/cGy]	2.53	4.51	3.25	0.52
$(D_{out}/D_{nom})_{HA}$ [MU/cGy]	1.74	2.68	2.05	0.23
T_B [min]	1.7	2.8	2.1	0.3
T_T [min]	17.0	33.0	24.8	4.0

V_{PTV} volume of PTV; $V_{90\%}$ and $V_{95\%}$ relative volume of V_{PTV} with at least 90 and 95% of prescribed dose; D_{min} minimum dose; $D_{98\%}$ near-minimum dose according to [23]; D_{mean} mean dose; $D_{50\%}$ median dose; $D_{2\%}$ near-maximum dose according to [23]; D_{max} maximum dose; $CI_{95\%}$ conformity index of isodose level 95% according to Eq. 2; *HI* homogeneity index according to Eq. 3; *IC* inhomogeneity coefficient according to Eq. 4; $SADG|_{10Gy}^{47.5Gy}$ spatially averaged dose gradient according to Eq. 9; $SADG|_{43\%}^{86\%}$ spatially averaged dose gradient between the relative isodose levels 86 and 43%; *GI* gradient index of the isodose levels 86 and 43% according to Eq. 10, $(D_{out}/D_{nom})_x$ dose ratio for the irradiation techniques x ∈ {DCA, IMRT, HA} according to Eq. 5; *DCA* dynamic conformal arcs; *IMRT* intensity-modulated static fields; *HA* HybridArc™; T_B beam-on time per fraction; T_T treatment session time

magnetic resonance imaging with and without contrast agent. Considering eye mobility, patient set-up error and machine tolerances, a safety margin of 2 to 3 mm was used according to previous publications which report on a margin of 3 mm being adequate for stereotactic radiotherapy with closed eyes [19]. We verified our safety margin conception by 120 intra-beam measurements of the tumour kinematics during IGRT.

All irradiations of the tumours were planned by the module HybridArc™ of the treatment planning system iPlan® RT Dose 4.5.3 (BRAINLAB AG, Feldkirchen, Germany). The first step of dose optimisation was always the manual adjustment of the geometry of non-coplanar DCAs with approximately 70% of the prescribed total dose. In a second step, the IMRT dose delivery of the remaining 30% of the prescribed dose was optimised with a maximum beamlet size of 2 mm in dynamic leaf sequencing and with tongue-and-groove optimisation by the optimiser DPL2i, version 4.5.

The applied dose calculation algorithm was BrainLAB PencilBeam X, which here used a kernel resolution of 0.63 mm. The dose grid size was 2 mm and finer for small objects; in normal tissue this value was set to 4 mm. The density artefacts—caused by the implanted tantalum markers of physical density 16.7 g/cm^3 needed for IGRT—in the native computer tomographs with 1 mm slice thickness and pitch factor 1 were corrected by the CT number 0 Hounsfield units (HU; 0 HU corresponds to electron density 0.998, relative to true water). This is a simple uniform approximation for the hypo- and hyperdense regions of such artefacts: the first type lies predominantly around the eyeball were the average density of tissue is roughly –50 HU; the second one we find directly around the markers within the eyeball where the "anatomical" density is about 50 HU.

Beam geometry

On average, a combination of five DCAs (range four to six) with six IMRT fields (range five to eight) provided by HA was used for treatment. Convenient arc lengths were 30 ° to 100 °; the couch angles had increments in the range of 15 ° to 60 °.

Quality of treatment plans

The characteristic properties and dose–volume metrics of the PTV are the absolute volume (V_{PTV}), the relative volume ($V_{x\%}$) with at least x% of the prescribed dose, the minimum (D_{min}), near-minimum ($D_{98\%}$), mean (D_{mean}), near-maximum ($D_{2\%}$) and maximum absorbed dose (D_{max}). Additionally, according to ICRU report 91, we reported the median absorbed dose ($D_{50\%}$) values which the half volumes of PTV and GTV received [20]. The definitions of the conformity indices (CI_{ICRU} and $CI_{x\%}$; [21, 22]), the homogeneity index (HI; [23]) and the inhomogeneity coefficient (IC; [24]) are

$$CI_{\mathrm{ICRU}} = \frac{V_{95\%}(PTV) + V_{95\%}(NT)}{V(PTV)} \geq 1, \tag{1}$$

$$CI_{x\%} = 1 + \frac{V_{x\%}(NT)}{V_{x\%}(PTV)} \geq 1, \tag{2}$$

$$HI = \frac{D_{2\%} - D_{98\%}}{D_{50\%}} \geq 0, \tag{3}$$

$$IC = \frac{D_{\max} - D_{\min}}{D_{\min}} \geq 0, \tag{4}$$

where NT stands for normal tissue. 2, 50 and 98% of the PTV receive at least the dose values $D_{2\%}$, $D_{50\%}$ and $D_{98\%}$, respectively.

HA spares output dose compared to pure IMRT; it needs only little more monitor units (MUs) than conformal open multi-leaf collimator (MLC) fields. The number of needed MUs not only affects the photon scattering and radiation protection, but also influences the beam-on (T_B) and treatment session time (T_T) per fraction. An evaluation criterion is the ratio of output dose to nominal tumour dose (D_{out}/D_{nom}). In general, the output dose of a linear accelerator can be calculated by

$$D_{\mathrm{out}} = \frac{D_{\mathrm{nom}} \cdot [SSD/(100\,\mathrm{cm})]^2}{D_{\mathrm{ref}} \cdot OF \cdot [PDD/(100\%)]}\,[MU]\,. \tag{5}$$

The ratio D_{out}/D_{nom} can be determined with given parameter values for the source–surface distance (SSD), reference dose (D_{ref}), output factor (OF) and percentage depth dose (PDD; [25]). Because all treatment planning systems for photon beam therapy and most of them for particle therapy calculate D_{out}, the wanted ratio is a known quantity.

Another quality criterion is the steepness of dose slope between the PTV and normal tissue. We defined a mean dose gradient as the difference quotient averaged over all spatial directions—called spatially averaged dose gradient (SADG) and given in Eq. 9. In order to do this, the PTV and irradiated volume (V_{ir}) were mathematically modelled as ellipsoids based on the real tumour geometry described by the axial and sagittal basal diameters $2 \cdot a$ and $2 \cdot b$, respectively, as well as by the thickness $2 \cdot c$. By summation of an equidistant safety margin $\Delta r_{PTV} > 0$, the volume

$$V^*_{\mathrm{PTV}} = \frac{4}{3} \cdot \pi \cdot (a + \Delta r_{\mathrm{PTV}}) \cdot (b + \Delta r_{\mathrm{PTV}}) \cdot (c + \Delta r_{\mathrm{PTV}}) = V_{\mathrm{PTV}} \tag{6}$$

of the inner ellipsoid is fitted to the real size (V_{PTV}) of PTV. We assume that most choroidal melanomas and their PTVs have lentiform shape. In 15 of all 25 cases the relative error

$$\varepsilon = \frac{V^*_{\mathrm{PTV}}(\Delta r_{\mathrm{PTV}} = 2\ \mathrm{mm}) - V_{\mathrm{PTV}}}{V_{\mathrm{PTV}}} \cdot 100\% \tag{7}$$

was element of [–12.5%, +12.5%]; the interval boundaries ±12.5% we took because for the 25 PTVs in the range of 0.42 to 3.37 cm^3, the volume differences after usual post processing by smoothing averaged 12.5%. Analogously, the volume

$$V^*_{ir} = \frac{4}{3} \cdot \pi \cdot (a + \Delta r_{ir}) \cdot (b + \Delta r_{ir}) \cdot (c + \Delta r_{ir}) = V_{ir} \tag{8}$$

of the outer ellipsoid is fitted to the irradiated volume (V_{ir}) by summation of another equidistant margin $\Delta r_{\Delta D} > 0$ to Δr_{PTV}, resulting in the sum $\Delta r_{ir} = \Delta r_{PTV} + \Delta r_{\Delta D}$. Finally, the quality criterion SADG is defined by

$$\mathrm{SADG}|_{D_2}^{D_1} = \left(\frac{\Delta D}{\Delta r}\right)_{\mathrm{avg}} = \frac{D_2 - D_1}{(r_2 - r_1)_{\mathrm{avg}}} = \frac{D_2 - D_1}{\Delta r_{\Delta D}} < 0, \tag{9}$$

whilst the estimated isodose level on the PTV boundary is D_1, and the isodose enclosing V_{ir} has the dose value D_2. The mathematically exact SADG is the quotient of the solid angle integral of the difference quotient in Eq. 9 and the entire solid angle $\Omega = 4 \cdot \pi$. We will compare our values for the SADG according to Eq. 9 with the results for the mathematically exact SADG and the common gradient index

$$GI = \frac{V_{PI(PTV)/2}}{V_{PI(PTV)}} > 2, \tag{10}$$

where $V_{PI(PTV)}$ is the volume enclosed by the prescription isodose of the PTV and $V_{PI(PTV)/2}$ the volume of the isodose on half dose level [17]. For better comparability, we used the same relative isodose levels to calculate both gradient measures: 86% at the boundary of PTV, which is the mean value of D_{min} in Table 2, and one half of this value.

To evaluate the treatment plan quality by HA for SRT of choroidal melanomas concerning the criteria CI, HI, SADG, GI and D_{out}/D_{nom}, we performed a benchmark experiment, depicted in the appendix, for SRS of brain metastases by means of conformal arcs.

Dose values in OARs and normal tissue

For hypofractionation, we have to determine tolerance dose values for the OARs. With the biologically effective dose (BED)

$$BED\,(TD) = TD_{\mathrm{norm}} \cdot \left(1 + \frac{d_{\mathrm{norm}}}{\alpha/\beta}\right) = TD \cdot \left(1 + \frac{TD/5}{\alpha/\beta}\right) \quad (11)$$

complying with the linear-quadratic model [25], the equivalent fractionation schemes, the tissue-dependent parameter ratio α/β of the cell survival curve, the dose per fraction ($d_{\mathrm{norm}} = 2\,\mathrm{Gy}$) and the tolerance dose of the normal fractionation (TD_{norm}), the tolerance dose (TD) for five fractions can be calculated by

$$TD = \frac{5 \cdot \alpha/\beta}{2} \cdot \left[-1 + \sqrt{1 + \frac{4}{5 \cdot \alpha/\beta} \cdot TD_{\mathrm{norm}} \cdot \left(1 + \frac{d_{\mathrm{norm}}}{\alpha/\beta}\right)}\right]. \quad (12)$$

We analysed the clinical dose criteria maximum dose and/or mean dose to compare the results with the specific tolerance dose values according to Eq. 12 in all ipsilaterally and medially located OARs, as well as in the contralateral eye. Furthermore, the values of the relative volume at tolerance dose *TD* (V_{TD}) for the ipsilaterally located OARs were determined. We evaluated the absolute volume of normal tissue (NT) with at least 10 Gy as irradiated volume ($V_{10\,\mathrm{Gy}}$).

Quality assurance

The patient-customized quality assurance program included the measurement of three-dimensional dose distributions by an Octavius® 4D phantom with a 1000$^{\mathrm{SRS}}$ dose detector array (PTW GmbH, Freiburg, Germany), which synchronously rotates with the gantry, the isocentre verification, and light field checks by means of target positioner overlays (BRAINLAB AG, Feldkirchen, Germany). The gamma analysis was done by means of VeriSoft®, version 6.1 (PTW GmbH, Freiburg, Germany), using the option second/third pass. The applied calculation parameters were 1 mm distance-to-agreement, 1% dose error with reference to the local absolute dose and 5% dose threshold. An extensive Winston–Lutz test, based on electronic portal imaging device (EPID) measurements, before each first therapy session is also part of our quality assurance program. The angles of the gantry, collimator, and couch are varied in full range with an increment of 30 ° in the process. The analysis of the test results runs fully automatically by a self-developed algorithm in MATLAB® R2007a (The MathWorks, Inc., Natick, MA, USA).

Image guidance

Before radiotherapy planning started, four ophthalmological tantalum markers (Altomed Ltd., Boldon, UK) were placed on the sclera, as used for PBT [26]. All patients were treated after specific instruction and training to avoid eye movements during beam-on time. Marker positioning was verified and corrected with ExacTrac® 6.0.6 and Robotics® 2.0 (all by BRAINLAB AG, Feldkirchen, Germany) prior to each beam fraction. If the calculated shifts of the six-D marker fusion were greater than the accuracy thresholds 0.5 mm and 0.5 ° of the X-ray verification, shifts to the robotic couch were applied. We used the verification results of six patients, 18 treatment sessions and 120 beams to validate our safety margin conception. A self-developed algorithm in MATLAB® R2007a transformed the geometrical information of the treatment plan for the tumour and marker positions together with the calculated shifts, while performing six-D marker fusion, into tumour movements in three principal axes.

Dose delivery

The daily dose fractions of 5.6 MV flattening filter-free photons were delivered with the BRAINLAB frameless radiosurgery system on a linear accelerator Novalis powered by TrueBeam™ STx (BRAINLAB AG, Feldkirchen, Germany and VARIAN Medical Systems, Inc., Palo Alto, CA, USA) with a dynamic high-definition MLC HD 120™. The maximum dose rates were 800 MU/min for the IMRT fields and 1400 MU/min for the DCAs.

Clinical outcome

To evaluate the clinical outcome, the rates of local disease control, enucleation, metastatic spread, mortality and complications—especially dry eye syndrome, keratitis, cataract, retinal detachment, as well as discopathy—were determined.

Results

The percentage of dose given by the DCAs was (66.4 ± 4.1)% (range of 55.0 to 73.0%). Fig. 2 shows the dose distributions of a combined dose shape by DCAs complemented with static IMRT fields for patient no. 17 from Table 1 in three orthogonal isocentre planes; Fig. 2d presents a dose profile above the line of measurement in Fig. 2a.

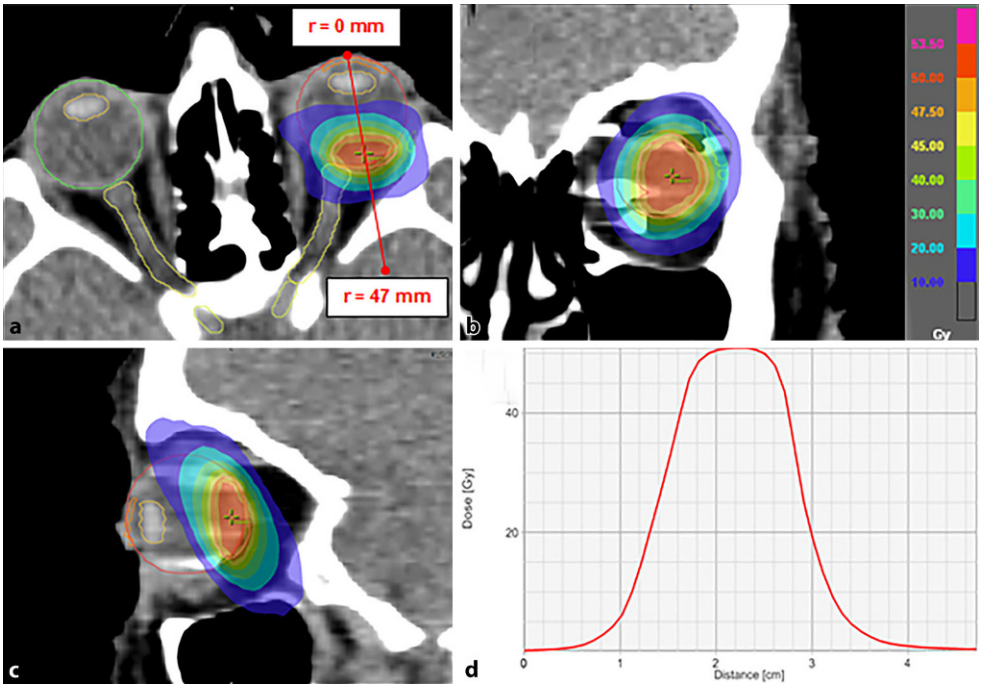

Fig. 2 Dose distribution calculated by iPlan® RT Dose 4.5.3 (BRAINLAB AG, Feldkirchen, Germany) in the region of the left eye with the choroidal melanoma of patient no. 17 from Table 1. The steepest dose fall-off is in the direction towards the ipsilateral lacrimal gland to avoid dry eye syndrome and not towards the optic nerve, which the tumour infiltrated. **a** Axial, **b** coronal and **c** sagittal isocentre plane. The segmented structures are the planning target volume (PTV) in magenta, lenses in yellow-orange, cornea in orange, eyeballs in red and green, optic nerves in yellow, as well as the chiasm in yellow-green. The dose range of the colour bar is 10.0 to 53.5 Gy or 20 to 107%. **d** The dose profile along the line r = (0 ... 47) mm in **a** has gradients of the stationary tangent up to 7.5 Gy/mm. The dose plateau in the region of the PTV illustrates the good dose homogeneity

Results for target volumes and tumours

We attempted to comply with the dose preconditions according to the ICRU report 62 for all PTVs: The maximum dose was less than 107% in all 25 cases and the criterion $V_{95\%}$, as a clinical metric for the minimum dose, was ≥98% in 17 cases [21]. The minimum, mean and maximum dose values in the PTVs were (86.0 ± 7.7)% (range 71.3–96.1%), (99.7 ± 0.3)% (range 99.2–100.1%) and (103.2 ± 0.9)% (range 101.7–105.1%) of the prescribed dose 50 Gy, respectively. The values of $CI_{95\%}$ according to Eq. 2 were 1.25 ± 0.15 (range 1.07–1.66). We received the values 0.08 ± 0.02 (range 0.04–0.13) for HI according to Eq. 3.

The values of median absorbed dose $D_{50\%}$ for the PTVs and GTVs were (100.5 ± 0.2)% (range 100.0–101.0%) and (101.1 ± 0.5)% (range 100.1–102.1%) of the prescribed dose, respectively. The minimum and maximum dose values in the GTVs were (98.9 ± 1.1)% (range 96.2–100.8%) and (103.0 ± 1.0)% (range 101.4–105.1%), respectively. In 12 of 25 cases (48%) the location of maximum dose was within the GTV. It was located inside the safety margins in 52% of all cases.

Quality of treatment plans

The values of the criterion $(D_{out}/D_{nom})_{HA}$ for HA were (2.05 ± 0.23) MU/cGy (range 1.74–2.68 MU/cGy). Of course, this result is worse than the values of $(D_{out}/D_{nom})_{DCA}$ for DCA but much better than the values of $(D_{out}/D_{nom})_{IMRT}$ for IMRT (confer Table 2).

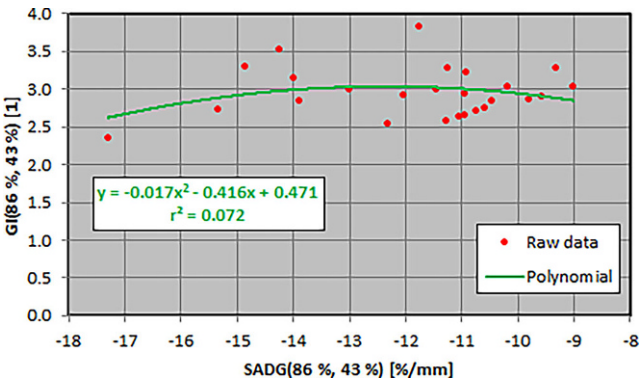

Fig. 3 Correlation between two dose gradient measures. *SADG(86%, 43%)* spatially averaged dose gradient between the relative isodose levels 86 and 43% according to Eq. 9, *GI (86%, 43%)* gradient index according to Eq. 10, $y = f(x)$ 2nd degree polynomial for the "function" GI = f(SADG), r^2 coefficient of determination for the nonlinear regression

Regarding the steepness of the dose fall-off between PTV and normal tissue as well as OARs, the achieved values of the criterion $SADG|_{10Gy}^{47.5Gy}$ according to Eq. 9 were (–3.5 ± 0.5) Gy/mm (range of –4.6 to –2.6 Gy/mm). We realised local dose gradients up to –11.5 Gy/mm to the directly adjacent OARs. The corresponding values of SADG with percentage dose in the unit (%/mm) are two times greater than the values with the unit (Gy/mm) because the nominal tumour dose is 50 Gy. We received the values 2.9 ± 0.3 (range 2.4–3.8) for the gradient index (GI) according to Eq. 10 for the isodose levels 86 and 43%. The values of $SADG|_{43\%}^{86\%}$ between the same isodose levels were (–11.9 ± 2.1)%/mm (range of –17.3 to –9.0%/mm). The coefficient of determination r^2 for linear and polynomial regressions of GI on SADG was ≤0.072; there was no significant correlation with meaningful regression (see Fig. 3). By contrast, we found a unique linear correlation between the approximated SADG according to Eq. 9 and the mathematically exact SADG. The coefficient of determination for the regression line of the approximated SADG on the exact SADG was 0.776. The relative error of the approximated versus exact SADG was (–4.5 ± 7.4)% (range of –19.3 to 8.3%).

Dose values in OARs and normal tissue

Table 3 summarises the achieved values for the clinical criteria mean dose (D_{mean}) and maximum dose (D_{max}) in comparison to the tolerance doses according to Eq. 12, as well as the relative volume V_{TD} with at least the tolerance dose (TD) for all ipsilaterally and medially located OARs. Statistical data for the absolute volume of normal tissue (NT) with at least 10 Gy ($V_{10\,Gy}$) and the maximum dose in the contralateral eye are also given in Table 3.

Table 3 Tolerance dose values, results and statistics for the dose–volume metrics describing the dose distributions in the ipsilaterally and medially located organs at risk, as well as the contralateral eye of 25 patients with choroidal melanomas

Organ at risk	TD_{norm} [Gy]	α/β [Gy]	TD [Gy]	Criterion	Minimum	Maximum	Mean value	Standard deviation
Bone	60	5	35.0	D_{max} [Gy]	15.3	50.0	27.8	10.0
Brain	30	3	20.9	D_{max} [Gy]	4.1	21.2	11.4	4.8
Brainstem	54	2	28.2	D_{max} [Gy]	0.1	4.5	0.7	0.9
Chiasm	54	2	28.2	D_{max} [Gy]	0.1	8.4	1.4	1.7
Cornea	30	2	20.0	D_{mean} [Gy]	0.2	19.8	2.1	3.9
				D_{max} [Gy]	0.8	44.9	9.0	11.1
				V_{TD} [%]	0.0	44.5	1.8	8.9
Eye contralateral	5[a]	1[a]	6.5[a]	D_{max} [Gy]	0.1	3.9	0.6	1.0
Eye without PTV	50	3	28.6	D_{mean} [Gy]	8.4	26.6	15.8	4.8
				D_{max} [Gy]	46.7	50.6	49.1	1.0
				V_{TD} [%]	6.0	43.2	19	9.9
Lacrimal gland	30	3	20.9	D_{mean} [Gy]	1.0	21.4	10.2	6.5
				D_{max} [Gy]	4.7	50.0	25.2	14.9
				V_{TD} [%]	0.0	53.4	11.1	16.4
Lens	5	1	6.5	D_{mean} [Gy]	0.7	48.1	5.6	10.2
				D_{max} [Gy]	2.4	51.4	14.9	15.4
				V_{TD} [%]	0.0	100.0	16.2	28.6
Macula	45	3	26.9	D_{max} [Gy]	7.7	50.7	41.8	12.6
Normal tissue	–	–	–	D_{max} [Gy]	49.1	51.0	50.0	0.5
				$V_{10\,Gy}$ [cm^3]	9.3	53.6	27.8	12.5
Optic nerve	54	2	28.2	D_{max} [Gy]	8.4	51.8	45.0	10.8
				V_{TD} [%]	0.0	38.9	13.1	9.8
Papilla	54	2	28.2	D_{max} [Gy]	8.4	51.8	45.0	10.8

TD_{norm} tolerance dose of the normal fractionation [32]; *α/β* tissue parameter ratio of the cell survival curve [32]; *TD* tolerance dose for SRT in five fractions according to Eq. 12; *D_{mean}* mean dose; *D_{max}* maximum dose; *V_{TD}* relative volume with at least the tolerance dose; *PTV* planning target volume; *$V_{10\,Gy}$* absolute volume of normal tissue with at least 10 Gy

[a]Valid for the lens, the most radiosensitive organ in eye

We achieved the mean dose values (10.2 ± 6.5) Gy (range 1.0–21.4 Gy) in the ipsilateral lacrimal gland. The maximum dose values in the ipsilateral macula lutea and papilla were (41.8 ± 12.6) Gy (range 7.7–50.7 Gy) and (45.0 ± 10.8) Gy (range 8.4–51.8 Gy), respectively. These dose metrics were also expressed as functions of the minimal distances between the OARs and the GTV, which are given in Table 1. We found second-degree polynomials with the coefficients of determination 0.676, 0.826 and 0.779 for the ipsilateral lacrimal gland, macula lutea and papilla, respectively.

The relative volumes which received at least the individual tolerance dose were (1.8 ± 8.9)% (range 0.0–44.5%), (19.0 ± 9.9)% (range 6.0–43.2%), (11.1 ± 16.4)% (range 0.0–53.4%), (16.2 ± 28.6)% (range 0.0–100.0%) and (13.1 ± 9.8)% (range 0.0–38.9%) for the ipsilateral cornea, healthy part of eye—including ciliary body, fovea centralis, and retina—lacrimal gland, lens and optic nerve, respectively.

The maximum dose values in the contralateral lacrimal gland, lens and optic nerve were within the ranges—defined by the mean values and standard deviations—(0.1 ± 0.0) Gy, (0.2 ± 0.2) Gy and (1.3 ± 1.2) Gy, respectively. The volumes of normal tissue irradiated with at least 10 Gy were (27.8 ± 12.5) cm^3 (range 9.3–53.6 cm^3). The maximum dose values in the contralateral eye were in the range (0.6 ± 1.0) Gy.

Quality of dose delivery

In all cases, the gamma analysis yielded high passing ratios of voxels with a gamma index $\gamma < 1$ relative to all evaluated voxels: (99.5 ± 0.3)% (range 98.9–100.0%). The local deviations between the measured phantom dose and the calculated dose in the particular isocentre, which was in principle nearly identical to the geometrical mass centre of the PTV, and of course a representative reference point in line with ICRU report 50 [27], were in the range of ±0.5%.

The isocentre verification and light field checks by means of target positioner overlays have shown geometric misalignments <0.3 mm. The analysis of one Winston–Lutz test for the gantry, collimator and couch angle reproducibly revealed for the isocentre coordinates $(X, Y, Z)_{ISO}$ according to IEC 61217 [28] the vectors (0.0, 0.0, 0.0) mm, (0.0, 0.3, 0.0) mm and (0.0, 0.1, 0.0) mm, respectively. The magnitudes, R_{max}(ISO), of the maximal spatial radius vector for the three angles were 0.4 mm, 0.4 mm and 0.3 mm, respectively. The corresponding maximums, D_{max}(ISO), of all diameters measured in the principal axes X, Y, and Z had the values 0.6 mm, 0.2 mm and 0.5 mm, respectively. The radiological isocentre of the patient positioning system ExacTrac® 6.0.6 was exactly located in the isocentre of the linear accelerator.

Table 4 Safety margins in three principal axes between GTV and PTV

Margin	ΔX [mm]	ΔY [mm]	ΔZ [mm]
GTV-ITV[a]	1.5	1.7	1.7
Δ_{IGRT}	0.5	0.5	0.5
Δ_{ISO}[b]	0.3	0.4	0.1
Total	2.3	2.6	2.3

GTV gross tumour volume; *PTV* planning target volume; *(ΔX, ΔY, ΔZ)* safety margins in the patient-fixed system of coordinates according to IEC 61217 [28] at couch angle 0 °; *ITV* internal target volume; Δ_{IGRT} positioning accuracy of image-guided radiotherapy by ExacTrac® (BRAINLAB AG, Feldkirchen, Germany); Δ_{ISO} maximal deviation of linac's centre beam relative to ideal isocentre

[a]For 2% significance level

[b]Only deviations of linac's isocentre for combined gantry and collimator rotations, because ExacTrac® detects and corrects the deviations in case of isocentric couch rotations

Validation of safety margins

The calculated tumour movements in the directions right-to-left (X), inferior-to-superior (Y) and posterior-to-anterior (Z) are summarised in the first data row of Table 4. These values represent with 98% confidence probability the safety margins between GTV and internal target volume (ITV). We received the total safety margins 2.3 mm, 2.6 mm and 2.3 mm in the directions X, Y and Z, respectively, together with the residual positioning error 0.5 mm of image guidance in a frameless workflow [29] as in the second data row of Table 4 and the deviations of linac's isocentre as in the third data row of Table 4.

Clinical outcome

After a median follow-up time of 19.6 months (range of 6.8 to 37.7 months), the local disease control rate was 100%. There was no case of enucleation. Two of 25 patients (8%) suffered from metastatic disease progression to the liver 12.4 and 19.9 months after the end of radiotherapy and died from metastatic disease. There were no severe complications. Two patients (8%) complained of eye dryness treated with artificial tear supplement. Transient keratitis was observed in three cases (12%). The rate of cataract was high with 13 of 25 patients (52%). Retinal detachment persisted in 19 cases (76%) after SRT. Three patients (12%) were diagnosed with radiation-induced discopathy.

Discussion

To evaluate the achieved treatment plan quality for SRT of choroidal melanomas by means of HA, we have to compare our results with previously reported data of studies which are based on the standard techniques PBT, SRS and SRT for ocular tumours. We used our own benchmark data in

the appendix for the assessment of quality criteria without available data for direct comparison.

Quality of treatment plans

The quality of treatment plans is paramount, and we followed the dose preconditions in the ICRU report 62 [21] and ICRU report 91 [20]. These recommendations are highly suitable, as they lead to robust treatment standards which make radiotherapy planning and dose delivery comparable and reproducible. Our maximum dose values comply with the ICRU report 62, and our minimum dose values at PTV boundary are obey ICRU report 91. The mean of all minimum dose values in PTV was, with 86.0%, less than the recommended 95.0% in the ICRU report 62, but the best possible coverage of PTV according to the individual clinical situation while optimally restricting absorbed dose to the planning organ-at-risk volumes like described in ICRU report 91.

We investigated the dependency of the mean dose values in the ipsilateral lacrimal gland, as well as the maximum dose values in the macula lutea and papilla on the minimal distances between these OARs and the tumour. We found quadratic correlations with strictly monotonically decreasing courses of the corresponding functions. The curve progressions were between a straight line with negative slope and a dose–distance characteristic in the manner of the inverse square law. Consequently, the dose optimiser realised distance-dependent dose gradients in direction to these OARs: the smaller the distance between OAR and tumour, the steeper the dose fall-off.

Because (66.4 ± 4.1)% of the therapeutic dose was given by means of DCAs, we inherently received steep dose gradients at the boundary of the PTV, which were locally improved by the IMRT fields of HA; the best value was –11.5 Gy/mm or –22.9%/mm. For comparison, the best local dose gradient of the benchmark experiment in the appendix with the 10 mm circular cone was –20.3%/mm. Furthermore, DCAs delivered highly conformal dose distributions at the tumour's boundary with low output dose; IMRT fields homogenized the absorbed dose in the PTV at the same time. Consequently, we obtained good values for the quality criteria $CI_{95\%}$, D_{out}/D_{nom} and HI.

The quality criteria HI and CI solely provide information regarding the dose distribution within the PTV and the encompassing isodose, respectively, but not outside the treated volume. For a complete description of the dose distribution within the irradiated volume, we introduced a novel quality criterion, termed SADG, which allows quantification of the dose fall-off at the PTV boundary. The assessment of the treatment plan quality is enhanced by the SADG. We found no significant correlation of the common gradient measure GI on SADG. In contrast, a significant correlation with meaningful linear regression between the utilized approximated SADG and the mathematically exact SADG was detected. GI was developed to measure dose gradients of Gamma Knife® irradiations for small cranial tumours, corresponding to a scenario where the isodose lines are approximately equidistant to the target volume surface. In SRT of ocular tumours, the need for locally steep dose gradients towards miscellaneous OARs results in deformed isodose lines with reduced and increased distances relative to the boundary of PTV. SADG is able to realise the anisotropy of dose gradients.

Challenges for photon beam therapy

High precision in radiotherapy requires sophisticated positioning control or implantation of fiducial markers. However, movements of the eye cannot be taken into account in real-time; therefore, robustness of plans remains a challenge for SRT and SRS of small targets. Based on the verification results during image guidance in 18 treatment sessions with 120 beams of six patients, we calculated the total safety margins 2.3 mm, 2.6 mm and 2.3 mm in a patient-fixed system of coordinates. Thus, the used safety margins in the range of 2 to 3 mm between GTV and PTV are appropriate. Consequently, the safety margins in the present series were –23 to –13% smaller than the recommended 3 mm margin reported previously for SRT of ocular melanomas with closed eyes under ideal set-up conditions [19]. With the restriction of the maximum dose throughout the PTV according to the ICRU report 62 [21], we ensure in our approach with closed, unfixed eyes, the best possible protection of OARs against absorbed dose.

We have shown that treatment planning by HA results in very good dose homogeneity within the PTV; this feature contributes to the robustness of plans. However, the complexity of treatment planning, IGRT and quality assurance required for photon beam therapy of ocular tumours by means of HA is challenging, even if the workflow is clinically robust and effective.

Comparison between HA and IMAT

To make certain that HA is a good choice of treatment technique for choroidal melanomas, we performed a comparative treatment planning study with a common treatment technique in SRT: intensity-modulated arc therapy (IMAT). Clearly, more sophisticated beam geometry achieved by HA—the predominant amount of fraction dose is applied by DCAs, which cause less scattered photons than intensity-modulated arcs—is superior to IMAT regarding the absorbed dose values in the OARs [30].

We also have investigated HA with respect to novel technologies as provided by premium vendors. We showed that

HA is superior to RapidPlan™ (VARIAN Medical Systems, Inc., Palo Alto, CA, USA) using multiple intensity-modulated partial arcs in terms of absorbed dose given to OARs even after optimising plans by automated planning [30].

Relation to the state of the art

Previously, comparative planning with photon beam therapy and PBT has been reported by Weber et al. [24]. The analysis was based on four hypothetical cases generated with predefined PTVs. In order to get an idea of the treatment planning quality by means of HA, we selected four comparable cases from Table 1 with respect to tumour and PTV sizes. Dosimetric comparison for PTVs and OARs was not possible due to missing anatomical data [24]. The results of the plan quality comparison are summarised in the appendix and in Table 6.

Reporting dose–volume metrics within the target volumes according to the ICRU reports 62 and 91 [20, 21] make treatment plans comparable and standards for dose escalation or de-escalation user independent. Indeed, dose inhomogeneity, especially locally excessive dose values within the PTV associated with closed, unfixed eyes, should be avoided to minimise the risk of complications such as radionecrosis, radiogenic maculopathy, papillopathy and optic neuropathy, in particular if the affected organs abut on or intersect the PTV [31].

With the ICRU report 91 uniform SRS and SRT standards have become available. But especially for ocular tumours, the optimal isodose level encompassing the PTV has not been decided on. Frequently, 70% was used in robotic SRS [8], and 80% has been recommended for linac-based photon beam therapy [7]. In our series, we realised minimal dose coverages in the range (86.0 ± 7.7)% (confer Table 2). It remains to be shown whether variable dose coverage of and homogeneity in the PTV are associated with the altered clinical outcome reported by others [7, 8].

Weakness of study and comparison method

Flaws of our work are reduced to the technically feasible and lie within the tolerance ranges of previous publications. Head-to-head comparison at this stage of application has not been possible. We acknowledge that precise dose delivery is achievable; however, the impact of dose optimising on clinical outcome remains unclear. The evaluation of the clinical outcome in our ocular tumour program will be assessed in a cohort analysis. So far, after a median follow-up of 19.6 months, the recent rates of local disease control, enucleation, metastatic spread and severe complications are encouraging: 100%, 0%, 8% and 0%, respectively. Because up to now only a few patients have a follow-up period of more than 3 years, an outcome comparison with the large studies about irradiation of ocular tumours by proton and photon beam therapy, as well as robotic SRS and Gamma Knife®, is not meaningful at the present time. Furthermore, it remains debatable whether controlled comparative trials of different radiation techniques are mandatory or feasible.

Another point of criticism is the comparison of our treatment planning results with previously published data of the gold standard with PBT or SRT. We only used two comparative criteria relating to dose conformity of and inhomogeneity within the PTV. The considered PTVs in each case could not be identical concerning dimensions and anatomical location, only the corresponding tumours and PTVs were of the same volume. In the relevant treatment planning study, no distances between the GTV and OARs were published [24].

Conclusion

Photons from linear accelerators are widely available. The combination of DCAs with static IMRT fields, termed HA, yields highly conformal dose distributions with steep dose gradients at the PTV boundary for the photon-based SRT of ocular tumours. The good dose homogeneity within PTV achieved by this treatment technique is with closed, unfixed eyes the best possible restriction of absorbed dose to parts of OARs which can reside within the safety margins during beam-on time. We are encouraged to pursue our ocular tumour treatment program with a workflow that minimises safety margins between tumour and PTV. The calculation of the novel quality criterion SADG should be implemented in all existing treatment planning systems because SADG gives more information on the global anisotropic dose fall-off towards normal tissue and OARs than GI.

Compliance with ethical guidelines

Conflict of interest M. Wösle, L. Krause, S. Sreenivasa, D. Vordermark and I.F. Ciernik declare that they have no competing interests.

Ethical standards Informed consent was obtained from all individual participants included in the study.

Appendix

Benchmark experiment for evaluating treatment plan quality

A good benchmark to compare dose conformity, homogeneity, gradient measures and the dose ratio D_{out}/D_{nom} is SRS of brain metastases. This thought experiment is simple, and all physicians and medical physicists with stereotaxy experience are able to ascertain it.

Table 5 Benchmark data of stereotactic radiosurgery for brain metastases for assessment purposes concerning treatment plan quality criteria in stereotactic radiotherapy for choroidal melanomas by means of HybridArc™ (BRAINLAB AG, Feldkirchen, Germany)

Choroidal melanomas	Brain metastases[a]													
Statistical quantity	V_{PTV} [cm³]	d_{PTV} [mm]	V_{PTV} [cm³]	Collimator	$CI_{80\%}$ [1]	HI [1]	D_{out}/D_{nom} [MU/cGy]	D_1 [%]	D_2 [%]	$\Delta r_{\Delta D}$ [mm]	$V(D_1)$ [cm³]	$V(D_2)$ [cm³]	SADG [%/mm]	GI [1]
Minimum	0.42	9.0	0.38	Cone[b]	1.01	0.20	1.56	74.0	37.0	1.99	0.51	1.41	–18.6	2.8
Mean value	1.83	15.0	1.77	MLC[c]	1.21	0.20	1.46	74.4	37.2	3.37	2.53	6.92	–11.0	2.7
Maximum	3.37	19.0	3.59	MLC[c]	1.18	0.19	1.41	79.2	39.6	3.80	4.35	11.33	–10.4	2.6
Mean value	1.87	14.3	1.91	–	1.13	0.20	1.48	75.9	37.9	3.06	2.46	6.55	–13.3	2.7
Standard deviation	1.48	5.0	1.61	–	0.11	0.01	0.08	2.9	1.4	0.95	1.92	4.97	4.6	0.1

V_{PTV} size of planning target volume (PTV); d_{PTV} diameter of PTV; *MLC* multi-leaf collimator; $CI_{80\%}$ conformity index of isodose level 80% according to Eq. 2; *HI* homogeneity index according to Eq. 3; D_{out}/D_{nom} dose ratio according to Eq. 5; D_1 isodose level at the boundary of PTV; D_2 half value of D_1; $\Delta r_{\Delta D}$ length of the difference vector in Eq. 9; $V(D_1)$ volume enclosed by the surface of isodose on level D_1; $V(D_2)$ volume enclosed by the surface of isodose on level D_2; *SADG* spatially averaged dose gradient between the isodose levels D_1 and D_2 according to Eq. 9; *GI* gradient index according to Eq. 10

[a]Location: temporo-parietal in the left hemisphere, 3 cm skin-to-centre of metastasis distance; dose calculation: iPlan® RT Dose 4.5.5, BrainLAB PencilBeam X; treatment parameters: 21 Gy single-dose, 5.6 MV flattening filter-free photons, five arcs, 160 ° arc length with cone, 120 ° arc length with MLC, 30 ° couch angle increment

[b]Circular cone diameter 10 mm (BRAINLAB AG, Feldkirchen, Germany)

[c]High-definition multi-leaf collimator HD 120™ of Novalis powered by TrueBeam STx # 1426 with 0.5 mm spatially equidistant field margin; no proper circular cone was available

For this experiment we generated treatment plans for spherical PTVs with highly conformal dose distributions. Three different PTVs were of equal size as the minimal, mean and maximal PTV in the cohort of 25 patients with choroidal melanomas. The results of our benchmark experiment to evaluate the novel dose gradient measure SADG according to Eq. 9 were summarised in Table 5. In Table 5, we also saw an unexpected characteristic of GI according to Eq. 10 on the PTV size: With increasing size of PTV, GI became better and SADG worsened. But only the characteristic of SADG is right, because with increasing field size the total physical penumbra broadens and as a result, the dose gradient at PTV boundary worsens.

The values of the criterion $CI_{95\%}$ according to Eq. 2 of our series in Table 2 were worse than the results for SRS obtained from assessments of the benchmark in Table 5: 1.25 ± 0.15 versus $CI_{80\%} = 1.13 \pm 0.11$. That is not surprising because in the benchmark, the convenient geometric and anatomical conditions—spherical PTV without adjacent OARs—allow almost ideal values for CI. However, the values for HI according to Eq. 3 of our series were twice as good as the values of the benchmark: 0.08 ± 0.02 versus 0.20 ± 0.01. Thus, the achieved values of $CI_{x\%}$ and HI were undoubtedly clinically acceptable in the present series. The corresponding values for the dose gradient measures SADG and GI were of the same order: (-11.9 ± 2.1)%/mm versus

Table 6 Tumour size, planning target volume size, conformity index and inhomogeneity coefficient for four choroidal melanomas from Table 1 in comparison with four virtual tumours of the treatment planning study [24]

Tumour no. in [24]	Volume [cm³]	PTV [cm³]	$CI_{ICRU}(X)$[a] [1]	$CI_{ICRU}(p^+)$[b] [1]	IC(X)[a] [1]	IC(p^+)[b] [1]	Patient no. in Table 1	GTV [cm³]	PTV [cm³]	CI_{ICRU}(HA) [1]	IC(HA) [1]
1	0.18	0.65	1.47	1.30	0.22	0.08	4	0.10	0.61	1.07	0.12
2	0.21	0.75	1.59	1.28	0.24	0.09	11	0.20	0.89	1.03	0.10
3	0.51	1.25	1.34	1.32	0.17	0.11	18	0.21	1.16	1.12	0.11
4	1.11	2.61	1.31	1.21	0.28	0.12	5	0.90	2.75	1.17	0.15
Median	0.36	1.00	1.41	1.29	0.23	0.10	Median	0.21	1.03	1.09	0.12

GTV gross tumour volume; *PTV* planning target volume; CI_{ICRU} conformity index according to Eq. 1, *X* high-energy photons, p^+ protons; *IC* inhomogeneity coefficient according to Eq. 4; *HA* HybridArc™ (BRAINLAB AG, Feldkirchen, Germany)

[a]The best value in each case of all three linac-based stereotactic photon beam techniques in [24]: static conformal fields, dynamic conformal arcs, and intensity-modulated radiotherapy

[b]The best value in each case of the two proton beam techniques in [24]: fixed horizontal proton beam and intensity-modulated spot-scanning proton therapy

(–13.3 ± 4.6)%/mm and 2.9 ± 0.3 versus 2.7 ± 0.1, respectively. The advantage for the benchmark in both gradient measures is—as stated before—a consequence of the more convenient geometric conditions. The values for D_{out}/D_{nom} according to Eq. 5 relating to the dose fraction applied by DCA in Table 2 were also confirmed by the benchmark experiment: 1.45 ± 1.10 versus 1.48 ± 0.08.

Comparison of treatment planning results with gold standard

In Table 6 we compared our treatment planning results with published results of the gold standard methods PBT and linac-based SRT [24] by means of the criteria CI_{ICRU} according to Eq. 1 and IC according to Eq. 4.

HA yields better plan qualities concerning dose conformity at the PTV boundary than the previously reported photon beam techniques, which have until now defined the standard in linac-based SRT. HA also seems competitive to PBT, because in the present series, the median of CI_{ICRU} for all four cases is 1.09, and thus closest to the optimum of 1.00. Undoubtedly, good conformity is one necessary precondition for dose sparing in normal tissue and OARs.

Another aspect is the maximum dose and dose inhomogeneity within the PTV. In the comparative study by Weber et al., the range was 109.0 to 130.0% for photon beam therapy and 101.0 to 115.0% for PBT [24]. Our maximum dose values with HA never exceeded 105.1% of the prescribed tumour dose. Expressed with values of IC, our median value 0.12 is closer to the optimum of 0.00 than any previously reported value for any photon beam technique.

References

1. Gesellschaft der Epidemiologischen Krebsregister in Deutschland und Robert Koch-Institut (2017) Krebs in Deutschland für 2013/2014, 11th edn. Robert Koch-Institut, Berlin
2. American Brachytherapy Society—Ophthalmic Oncology Task Force (2014) The American Brachytherapy Society consensus guidelines for plaque brachytherapy of uveal melanoma and retinoblastoma. Brachytherapy 13(1):1–14
3. Krause L, Mladenova A, Bechrakis NE, Kreusel KM, Plath T, Moser L, Foerster M (2009) Treatment modalities for conjunctival melanoma. Klin Monbl Augenheilkd 226(12):1012–1016
4. Collaborative Ocular Melanoma Study Group (2006) The COMS randomized trial of iodine 125 brachytherapy for choroidal melanoma: V. Twelve-year mortality rates and prognostic factors: COMS report no. 28. Arch Ophthalmol 124(12):1684–1693
5. Hrbacek J, Mishra KK, Kacperek A, Dendale R, Nauraye C, Auger M, Herault J, Daftari IK, Trofimov AV, Shih HA, Chen YL, Denker A, Heufelder J, Horwacik T, Swakoń J, Hoehr C, Duzenli C, Pica A, Goudjil F, Mazal A, Thariat J, Weber DC (2016) Practice patterns analysis of ocular proton therapy centers: the international OPTIC survey. Int J Radiat Oncol Biol Phys 95(1):336–343
6. Modorati G, Miserocchi E, Galli L, Picozzi P, Rama P (2009) Gamma knife radiosurgery for uveal melanoma: 12 years of experience. Br J Ophthalmol 93(1):40–44
7. Dunavoelgyi R, Dieckmann K, Gleiss A, Sacu S, Kircher K, Georgopoulos M, Georg D, Zehetmayer M, Poetter R (2011) Local tumor control, visual acuity, and survival after hypofractionated stereotactic photon radiotherapy of choroidal melanoma in 212 patients treated between 1997 and 2007. Int J Radiat Oncol Biol Phys 81(1):199–205
8. Eibl-Lindner K, Fürweger C, Nentwich M, Foerster P, Wowra B, Schaller U, Muacevic A (2016) Robotic radiosurgery for the treatment of medium and large uveal melanoma. Melanoma Res 26(1):51–57
9. Kreusel KM, Bechrakis N, Riese J, Krause L, Wachtlin J, Foerster MH (2006) Combined brachytherapy and transpupillary thermotherapy for large choroidal melanoma: tumor regression and early complications. Graefes Arch Clin Exp Ophthalmol 244(12):1575–1580
10. Jang BS, Chang JH, Oh S, Lim YJ, Kim IH (2017) Surgery vs. radiotherapy in patients with uveal melanoma: Analysis of the SEER database using propensity score matching and weighting. Strahlenther Onkol 193(11):931–942
11. Bekkering GE, Rutjes AW, Vlassov VV, Aebersold DM, von Bremen K, Jüni P, Kleijnen J (2009) The effectiveness and safety of proton radiation therapy for indications of the eye: a systematic review. Strahlenther Onkol 185(4):211–221
12. Lin AJ, Rao YJ, Acharya S, Schwarz J, Rao PK, Grigsby P (2017) Patterns of care and outcomes of proton and eye plaque brachytherapy for uveal melanoma: review of the National Cancer Database. Brachytherapy 16(6):1225–1231
13. Beliveau-Nadeau D, Callejo S, Roberge D (2016) Technique for robotic stereotactic irradiation of choroidal melanoma. Cureus 8(4):e582
14. Klingenstein A, Kufeld M, Wowra B, Muacevic A, Fürweger C, Schaller UC (2012) CyberKnife radiosurgery for the treatment of orbital metastases. Technol Cancer Res Treat 11(5):433–439
15. Haas A, Pinter O, Papaefthymiou G, Weger M, Berghold A, Schröttner O, Müllner K, Pendl G, Langmann G (2002) Incidence of radiation retinopathy after high-dosage single-fraction gamma knife radiosurgery for choroidal melanoma. Ophthalmology 109(5):909–913
16. Robar JL, Thomas C (2012) Hybridarc: a novel radiation therapy technique combining optimized dynamic arcs and intensity modulation. Med Dosim 37(4):358–368
17. Paddick I, Lippitz B (2006) A simple dose gradient measurement tool to complement the conformity index. J Neurosurg 105(Suppl):194–201
18. Kaiser PK, Friedman NJ, Pineda R (2014) The massachusetts eye and ear infirmary—illustrated manual of ophthalmology, 4th edn. Elsevier Saunders, New York
19. Miralbell R, Caro M, Weber DC, Elizalde J, Perez-Ochoa A, Villà S, IgnacioToscas J, Martinez P, Linero D, Nouet P, Escudé L (2007) Stereotactic radiotherapy for ocular melanoma: initial experience using closed eyes for ocular target immobilization. Technol Cancer Res Treat 6(5):413–417
20. International Commission on Radiation Units and Measurements (2014) ICRU Report 91: prescribing, recording, and reporting of stereotactic treatments with small photon beams. J Int Comm Radiat Unit Meas 14(2):1–160. https://doi.org/10.1093/jicru/ndx017
21. Landberg T, Chavaudra J, Dobbs J, Gerard JP, Hanks G, Horiot JC, Johansson KA, Möller T, Purdy J, Suntharalingam N, Svensson H (1999) ICRU Report 62: prescribing, recording and reporting photon beam therapy (Supplement to ICRU Report 50). J Int Comm Radiat Units Meas 32(1):1–52
22. Ohtakara K, Hayashi S, Hoshi H (2012) The relation between various conformity indices and the influence of the target coverage difference in prescription isodose surface on these values in intracranial stereotactic radiosurgery. Br J Radiol 85(1014):e223–e228

23. International Commission on Radiation Units and Measurements (2010) ICRU Report 83: prescribing, recording, and reporting intensity-modulated photon-beam therapy (IMRT). J Int Comm Radiat Units Meas 10(1):1–106
24. Weber DC, Bogner J, Verwey J, Georg D, Dieckmann K, Escudé L, Caro M, Pötter R, Goitein G, Lomax AJ, Miralbell R (2005) Proton beam radiotherapy versus fractionated stereotactic radiotherapy for uveal melanomas: a comparative study. Int J Radiat Oncol Biol Phys 63(2):373–384
25. Podgorsak EB (2005) Radiation oncology physics: a handbook for teachers and students. International Atomic Energy Agency, Vienna
26. Lipski AC, Lakotka N, Riechardt AI, Willerding GD, Heufelder J, Türkmen S, Keilholz U, Moser UL, Joussen AM (2013) Diagnostik und Therapie choroidaler Melanome. Klin Monbl Augenheilkd 230(10):1005–1019
27. Landberg T, Chavaudra J, Dobbs J, Hanks G, Johansson KA, Möller T, Purdy J (1993) ICRU Report 50: prescribing, recording and reporting photon beam therapy. J Int Comm Radiat Units Meas 26(1):1–72
28. International Electrotechnical Commission (2007) Radiotherapy equipment—coordinates, movements and scales (IEC 61217:1996 plus A1:2000 plus A2:2007). VDE Verlag GmbH, Berlin
29. Gevaert T, Verellen D, Tournel K, Linthout N, Bral S, Engels B, Collen C, Depuydt T, Duchateau M, Reynders T, Storme G, De Ridder M (2012) Setup accuracy of the Novalis ExacTrac 6DOF system for frameless radiosurgery. Int J Radiat Oncol Biol Phys 82(5):1627–1635
30. Ciernik IF, Wösle M, Krause L, Krayenbuehl J (2018) Optimizing radiosurgery with photons for ocular melanoma. Phys Imag Radiat Oncol 6:83–88. https://doi.org/10.1016/j.phro.2018.06.001
31. Höcht S, Stark R, Seiler F, Heufelder J, Bechrakis NE, Cordini D, Marnitz S, Kluge H, Foerster MH, Hinkelbein W (2005) Proton or stereotactic photon irradiation for posterior uveal melanoma? A planning intercomparison. Strahlenther Onkol 181(12):783–788
32. Herrmann T, Baumann M, Dörr W (2005) Klinische Strahlenbiologie—kurz und bündig, 4th edn. Elsevier Urban & Fischer, München, Jena